

# Bioactive Nanoparticle–Gelatin Composite Scaffold with Mechanical Performance Comparable to Cancellous Bones

Chen Wang,<sup>†,‡</sup> Hong Shen,<sup>†</sup> Ye Tian,<sup>§</sup> Yue Xie,<sup>†</sup> Ailing Li,<sup>\*,†</sup> Lijun Ji,<sup>||</sup> Zhongwei Niu,<sup>§</sup> Decheng Wu,<sup>†</sup> and Dong Qiu<sup>\*,†</sup>

<sup>†</sup>Beijing National Laboratory for Molecular Sciences, State Key Laboratory of Polymer Physics and Chemistry, Institute of Chemistry, Chinese Academy of Sciences, Beijing 100190, China

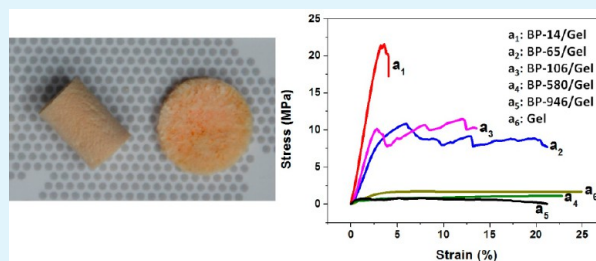
<sup>§</sup>National Research Centre of Engineering Plastics, Technical Institute of Physics and Chemistry, Chinese Academy of Sciences, Beijing 100190, China

<sup>‡</sup>University of Chinese Academy of Sciences, Beijing 100190, China

<sup>||</sup>College of Chemistry and Chemical Engineering, Yangzhou University, Yangzhou 225002, China

**ABSTRACT:** Mechanical properties are among the most concerned issues for artificial bone grafting materials. The scaffolds used for bone grafts are either too brittle (glass) or too weak (polymer), and therefore composite scaffolds are naturally expected as the solution. However, despite the intensive studies on composite bone grafting materials, there still lacks a material that could be matched to the natural cancellous bones. In this study, nanosized bioactive particles (BP) with controllable size and good colloidal stability were used to composite with gelatin, forming macroporous scaffolds. It was found that the mechanical properties of obtained composite scaffolds, in terms of elastic modulus, compressive strength, and strain at failure, could match to that of natural cancellous bones. This is ascribed to the good distribution of particle in matrix and strong interaction between particle and gelatin. Furthermore, the incorporation of BPs endues the composite scaffolds with bioactivity, forming HA upon reacting with simulated body fluid (SBF) within days, thus stimulating preosteoblasts attachment, growth, and proliferation in these scaffolds. Together with their good mechanical properties, these composite scaffolds are promising artificial bone grafting materials.

**KEYWORDS:** composite scaffold, bioactive nanoparticle, gelatin, mechanical property, cancellous bone



## 1. INTRODUCTION

Bone tissue loss and damage caused by injuries or diseases have emerged as one of the most troubling problems that jeopardize human health.<sup>1–3</sup> However, current substitutes including autografts, allografts, and xenografts are not satisfactory because of limited availability, donor site morbidity, immune reaction, risk of infection, etc.<sup>4–6</sup> Thus, artificial bone grafts are in high demand.<sup>7–9</sup> There are currently many bone graft substitute materials such as inorganic materials (hydroxyapatite (HA), bioactive glass, etc.)<sup>1,5,6,10</sup> and biodegradable polymers (poly(lactic acid) (PLA), poly lactic-co-glycolic acid (PLGA), gelatin, etc.).<sup>5,11,12</sup> However, none of the above materials could meet all the demands of a bone graft alone, especially for the mechanical properties. Composites of inorganic material and polymer are therefore expected to match the requirements in mechanical properties for bone substitutes.<sup>2</sup>

HA has been used for bone repair for many years, which is mainly due to its chemical and biological similarities to the mineral phase of the native bones. Composites of HA and polymers such as PLA/HA and PLGA/HA have been designed to improve the brittleness of HA.<sup>11,12</sup> However, poor mechanical properties have been found for these composites

because of the agglomeration of the HA particles in the polymer matrix and the weak adhesion between the hydrophilic HA and hydrophobic polymer.<sup>12–14</sup> For example, when the HA content is 50 wt %, the compression modulus and the yield strength of PLA/HA composite were only 9.87 and 0.44 MPa, respectively,<sup>11</sup> which cannot meet the demands of the bone grafts.

Bioactive silicate glass is a promising artificial bone grafting material as it has excellent osteoconductivity and bioactivity, the ability to deliver cells, and controllable biodegradability.<sup>10,15</sup> However, compared to natural bones, scaffolds of bioactive silicate glass lack the required mechanical properties, especially the toughness.<sup>16</sup> Similarly, incorporating the glass with a polymer to fabricate a composite is an easy and feasible solution. There have been many studies on polymer/glass composites as bone grafting materials.<sup>17–21</sup> It was found that with 75 wt % Bioglass, the Young's modulus of PLGA/45S5 Bioglass composites could be doubled compared to PLGA;

Received: May 13, 2014

Accepted: July 21, 2014

Published: July 21, 2014

nevertheless, there was little improvement in compressive strength ( $\sim 0.42$  MPa), which was far below the requirement for the bone grafts.<sup>18</sup> Besides the conventional micrometer-sized particles, nanosized bioactive particles (nBP) were also used with expectation for better mechanical performances.<sup>1,19,20</sup> Composite scaffold of nBPs  $\sim 40$  nm and polycaprolactone showed modulus and compressive strength up to 49.4 and 1.45 MPa, respectively, at a rather high nBPs concentration of 90 wt %.<sup>21</sup> nBPs (less than 80 nm in diameter) enhanced gelatin composite scaffolds could reach a modulus of 78 MPa and a compressive strength of 5.6 MPa.<sup>10</sup> However, these scaffolds only meet the minimum requirements in mechanical strength for cancellous bones (4–12 MPa), further improvements are still needed. It is worth noting that the nBPs used above often form aggregates in polymer matrix, which may reduce the interaction between particle and polymer, therefore limiting the improvement in mechanical properties of composite materials. From these reported studies, it seems to suggest that small particles are better in improving the mechanical performance of composite scaffolds, thus nBPs would be preferred, especially those which could be distributed well in polymer matrix.

Up to date, the preparation of monodisperse nBPs is still challenging, especially for particles with only a few tenths of nanometers.<sup>22–24</sup> In our previous work, monodisperse bioactive particles (BP) with controllable sizes and narrow size distribution were synthesized through surface modification of colloidal silica nanoparticles.<sup>25</sup> These BPs showed good colloidal stability and bioactivity, and thus are ideal model particles to investigate the size effect of BPs on the enhancement of scaffold mechanical property and bioactivity etc. In this study, BPs of different sizes were used as fillers to form composite scaffolds with gelatin, which was chosen as the matrix because of its excellent biodegradability, biocompatibility, cell adhesion and proliferation, resistance to immunogenicity, pathogen transmission, etc.<sup>26–29</sup> The resultant composite scaffolds were found to show mechanical properties comparable to cancellous bones, good bioactivity, and cytocompatibility.

## 2. MATERIALS AND METHODS

**2.1. BP/gelatin Composite (BP/gel) Scaffold Preparation.** BPs with mean diameters of 14, 65, 106, 580, and 946 nm (denoted as BP-14, BP-65, BP-106, BP-580, and BP-946, respectively) were synthesized using a modified sol–gel method.<sup>25</sup> The resultant BPs were dispersed in water at a concentration of 20 wt % before use.

Gelatin solution (20 wt %) was prepared by dissolving gelatin (Type A from porcine skin, Sigma-Aldrich) in water at 40 °C for 1 h. The BP dispersions were mixed with gelatin solution under stirring at 40 °C for 8 h. The mixtures were casted into polyethylene molds and aged for 24 h, followed by freezing for 8 h. The frozen samples were then stored at  $-54$  °C for 3 h, then freeze-dried for 3 days. The freeze-dried samples were then soaked in glutaraldehyde–water solution (1 wt %) for 24 h to form cross-linked scaffolds, which were further soaked in water for 48 h, with water changes every 8 h, to remove residual glutaraldehyde. Finally, porous composite scaffolds were obtained by freeze-drying for another 3 days. Porous gelatin (gel) scaffolds were also fabricated following the same procedure. The porous scaffolds of gel and BP/gel were kept in a dryer for further use. The information on the samples is summarized in Table 1.

**2.2. Physicochemical Structure Characterizations.** The morphologies of BPs were investigated by TEM (JEM 2011, JEOL, Japan). The densities and porosities of obtained scaffolds were measured using a liquid displacement technique.<sup>30</sup> Five samples were used in each composition to ensure the reproducibility. The

**Table 1. Information of Gel and BP/gel Scaffolds**

|            | BP (g) | gelatin (g) |               | BP-14 (g) | gelatin (g) |
|------------|--------|-------------|---------------|-----------|-------------|
| BP-14/gel  | 5      | 5           | BP-14-0.1/gel | 0.5       | 5           |
| BP-65/gel  | 5      | 5           | BP-14-0.2/gel | 1.0       | 5           |
| BP-106/gel | 5      | 5           | BP-14-0.5/gel | 2.5       | 5           |
| BP-580/gel | 5      | 5           | BP-14-1/gel   | 5.0       | 5           |
| BP-946/gel | 5      | 5           | gel           |           | 5           |

microstructure of gel and BP/gel scaffolds were investigated by SEM (JSM6700, JEOL, Japan).

**2.3. Measurement of Mechanical Properties.** Uniaxial compression tests were performed on an Instron 3365 mechanical testing machine with a 5 kN load cell under a cross-head speed of 1 mm·min<sup>-1</sup> until failure. Samples for mechanical testing were cylinders with a diameter of 6 mm and a height of 15 mm. The elastic modulus (*E*) was determined from the elastic region of stress–strain curves. Five samples were measured for each composition to check the reproducibility.

**2.4. In Vitro Bioactivity.** The ability of the porous BP/gel scaffolds to stimulate the formation of hydroxyapatite (HA) in vitro was investigated by soaking samples in the simulated body fluid (SBF) at a PH of 7.40 and temperature of 36.5 °C.<sup>26</sup> The samples (3 mg mL<sup>-1</sup>) were immersed in the SBF for 7 or 14 days, then washed with pure water three times to remove the unreacted ions. The in vitro bioactivity (formation of HA) of the samples was investigated by XRD after vacuum-dried for 3 days at room temperature.

**2.5. Cell Compatibility.** **2.5.1. Cell Culture.** A preosteoblast cell line (MC3T3-E1; ATCC, CRL-2593, Rockville, MD, USA) was seeded in the porous BP/gel scaffolds to investigate the cell compatibility in vitro. BP-14/gel, BP-65/gel, and BP-106/gel scaffolds were chosen as they may have better mechanical properties.<sup>31,32</sup> The MC3T3-E1 cells were cultured in a humidified incubator under an atmosphere containing 5% CO<sub>2</sub> at 37 °C. Dulbecco's Modified Eagle Medium (DMEM) supplemented with fetal bovine serum (FBS, 10%), penicillin (100 U cm<sup>-3</sup>), and streptomycin (100 U cm<sup>-3</sup>) was used as the culture medium. When the cells had grown to confluence, they were detached using trypsin/EDTA (0.05% (w/v) trypsin/0.02% (w/v) EDTA). Then, the cells were suspended in fresh culture medium for seeding into scaffolds.<sup>19,33</sup>

**2.5.2. Cell Morphology.** The disclike scaffolds for cell seeding were 15 mm in diameter and 1.5 mm in thickness. First, the scaffolds were disinfected in 70% ethyl alcohol solution for 2 h, washed twice in sterile PBS for 30 min, and then sterilized under high-intensity UV radiation for 4 h.<sup>34</sup> Afterward, the scaffolds were placed in a 24-well culture plate. MC3T3-E1 cell suspension (10 000 cells per well) was cultured in scaffold for 2 or 7 days. Then, the cell-scaffolds were washed with PBS, and fixed with 2.5% glutaraldehyde at 4 °C for 24 h. The cell-scaffolds were dehydrated using ethanol solutions (50, 75, 95, and 100 wt %), freeze-dried, and observed by SEM.

**2.5.3. Cell Proliferation.** After MC3T3-E1 cells were cultured in scaffolds for 1, 2, and 7 days, the cell viability and proliferation were determined by MTT assay.<sup>35,36</sup> The disclike scaffolds for the MTT assay were 5 mm in diameter and 2 mm in thickness. Scaffolds were placed in a 96-well culture plate and MC3T3-E1 cell suspension (10 000 cells per well) was poured into each well. The cells cultured in 96-well without scaffold were used as control. Similarly, the scaffolds were disinfected and sterilized before seeding as described above. At each predetermined interval, 300  $\mu$ L of fresh culture medium was added to each well after the original culture medium was removed. Then 8  $\mu$ L of MTT solution (5 mg mL<sup>-1</sup> in PBS) was added to each well, followed by incubation at 37 °C with 5% CO<sub>2</sub> for 4 h. The upper medium was removed carefully and the intracellular formazan was dissolved in 300  $\mu$ L of 0.04 mol L<sup>-1</sup> HCl/isopropanol. The absorbance of produced formazan was measured at 570 nm with microplate reader (ZS-2, Beijing).<sup>32</sup> Five species for each condition were tested to obtain the mean value and standard deviation.

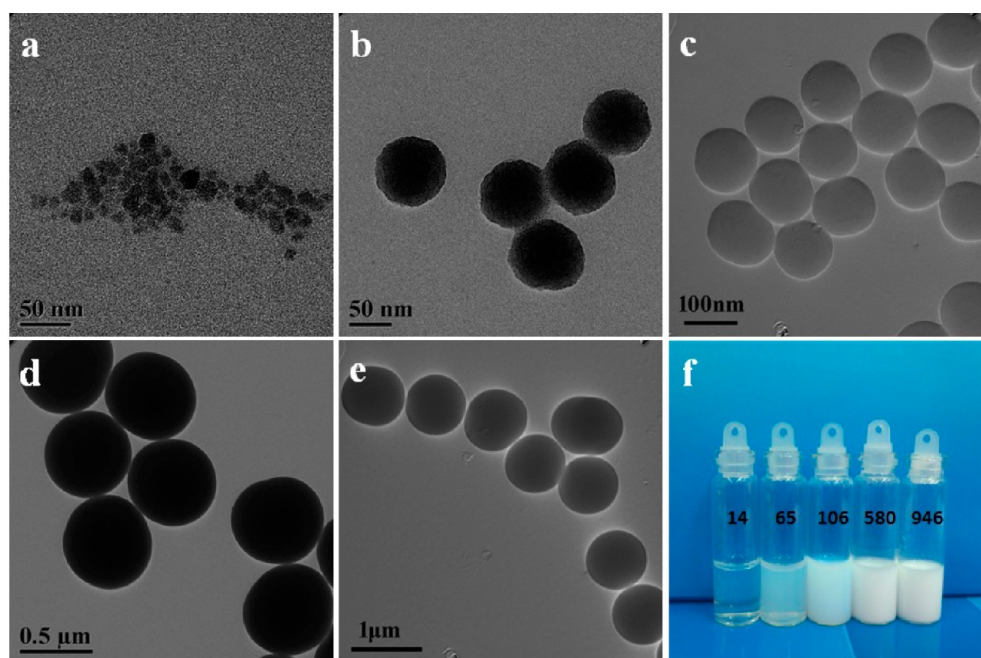


**Figure 1.** TEM images for BPs: (a) BP-14, (b) BP-65, (c) BP-106, (d) BP-580, and (e) BP-946; and (f) optical image of BP dispersions with different nominal diameters.

### 3. RESULTS AND DISCUSSION

**3.1. BP Characterization.** Monodisperse BPs with controllable size were synthesized according to reported procedures (Figure 1).<sup>25</sup> On the basis of TEM images, the average diameter of these BPs is  $14 \pm 8$ ,  $65 \pm 4$ ,  $106 \pm 6$ ,  $580 \pm 9$ , and  $946 \pm 10$  nm, respectively. As expected, at a small size, BPs show a bit irregular shape and broader size distribution (Figure 1a). At larger sizes, BPs are in nearly perfect spherical and with very narrow size distributions (Figure 1b–e). BPs have maintained good colloidal stability after storage up to weeks (Figure 1f), which is essential to ensure these particles distributing evenly when incorporated into polymer matrix by the solution blending approach.

**3.2. Composite Scaffold Morphology.** Composite scaffolds of BP/gel with well-defined macro pores were fabricated using a freeze-drying method. The optical image of BP-14/gel scaffolds is shown in Figure 2. It can be seen that composite scaffolds can be easily shaped by changing molds.

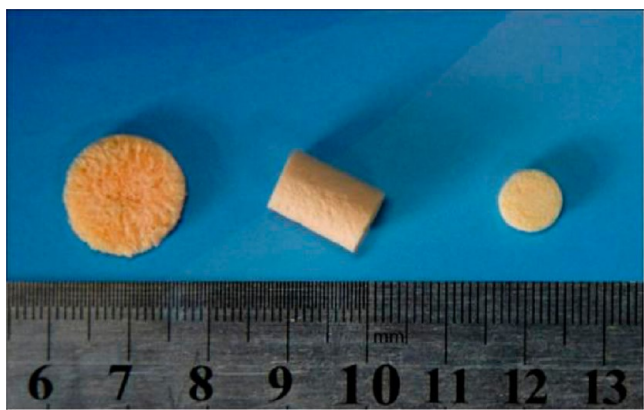


**Figure 2.** Optical images for BP-14/gel scaffolds made in different molds.

The microstructure of obtained composite scaffolds was investigated using SEM (Figure 3). It can be seen that the BP/gel composite scaffolds had open pores with a high degree of interconnectivity, very similar to the gel scaffold. The pore sizes of the composite scaffolds were in the range of 50 to 300  $\mu\text{m}$ , which is suitable for cell adhesion and growth as well as blood vessels growth.<sup>1,4,9</sup> With higher magnification, it can be seen that the BPs were also partially exposed on the wall of scaffolds (Insets in Figure 3), which was rather important, because the exposure of BPs enabled their direct contact with body fluid in the pores thus to show their bioactivity. On the contrary, when BPs are encapsulated by polymer, there normally is an induction period before the materials showing bioactivity.<sup>37</sup> The composite scaffolds had low apparent densities ( $\rho$ ) and high porosities (Table 2). In particular, BP-14/gel, BP-65/gel, and BP-106/gel scaffolds had porosities  $\sim 80\%$  and densities below  $0.4 \text{ g cm}^{-3}$ , meeting the requirements for cancellous bone grafts.

**3.3. Mechanical Properties.** Artificial bone grafts that can help the regeneration of bone as well as share load with surrounding bone in a bone defect are highly demanding. Therefore, the synthetic bone grafts should own similar mechanical properties to the surrounding bone tissues, so that the scaffold can withstand the in vivo conditions and share the load with the surrounding bone tissues.<sup>2</sup> Addition of BPs led to a remarkable improvement of the mechanical properties of the scaffolds, and smaller particles generally gave better reinforcement (Figure 4a). At the same particle loading, BP-14, BP-65, and BP-106 significantly enhanced the mechanical performance of the scaffolds while BP-580 and BP-946 only had marginal effect (Figure 4a). It can be found that the  $E$  could be higher than 300 MPa and yield strength ( $\sigma_{\text{yield}}$ ) higher than 10 MPa for BP-14/gel, BP-65/gel, and BP-106/gel scaffolds, fulfilling the requirements for cancellous bone substitutes (Table 2). Additionally, the yield strain ( $\epsilon_{\text{yield}}$ ) of those three samples was also found to be similar to the cancellous bone, adding further strength for their application as

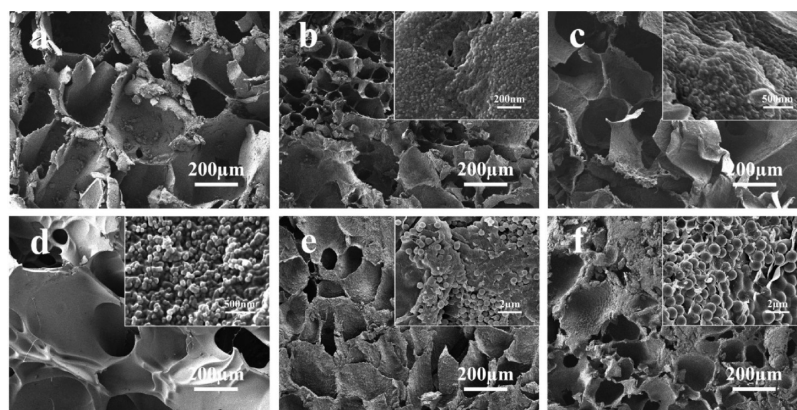


**Figure 3.** SEM images for gel and BP/gel scaffolds: (a) gel; (b) BP-14/gel; (c) BP-65/gel; (d) BP-106/gel; (e) BP-580/gel, and (f) BP-946/gel. The insets are higher magnifications.

**Table 2. Physicochemical and Mechanical Properties of BP/Gel Scaffolds**

| sample                       | $E$ (MPa)                         | $\sigma_{\text{yield}}$ (MPa) | $\epsilon_{\text{yield}}$ (%) | porosity (%)   | $\rho$ (g cm <sup>-3</sup> ) |
|------------------------------|-----------------------------------|-------------------------------|-------------------------------|----------------|------------------------------|
| compact bone <sup>a</sup>    | $3 \times 10^3$ – $3 \times 10^4$ | 130–180                       | 1–3                           | 5–30           | 1.8–2                        |
| cancellous bone <sup>a</sup> | 20–500                            | 4–12                          | 5–7                           | 30–90          | 0.14–1.2                     |
| gel                          | $47.2 \pm 16.3$                   | $1.8 \pm 0.2$                 | $5.1 \pm 1.2$                 | $85.1 \pm 1.2$ | $0.12 \pm 0.02$              |
| BP-14/gel                    | $602.3 \pm 73.4$                  | $15.4 \pm 2.5$                | $4.0 \pm 0.8$                 | $79.9 \pm 1.2$ | $0.39 \pm 0.10$              |
| BP-65/gel                    | $319.8 \pm 28.1$                  | $10.9 \pm 1.8$                | $6.2 \pm 1.4$                 | $85.1 \pm 2.4$ | $0.10 \pm 0.08$              |
| BP-106/gel                   | $409.3 \pm 53.6$                  | $10.5 \pm 1.7$                | $3.4 \pm 0.8$                 | $81.0 \pm 2.6$ | $0.25 \pm 0.07$              |
| BP-580/gel                   | $82.4 \pm 33.2$                   | $2.1 \pm 0.5$                 | $1.3 \pm 0.5$                 | $78.6 \pm 3.2$ | $0.12 \pm 0.05$              |
| BP-946/gel                   | $140.7 \pm 22.1$                  | $0.8 \pm 0.2$                 | $1.2 \pm 0.3$                 | $61.2 \pm 5.9$ | $0.17 \pm 0.11$              |

<sup>a</sup>The physicochemical and mechanical properties of compact and cancellous bones were quoted from ref 10.

potential bone grafts. It is interesting to note that at the same particle loading (10 wt %) and porosity (~80%), BP-106/gel exhibited significantly improved mechanical properties compared to composite scaffolds of gelatin with conventional sol-gel prepared bioactive glass particles (CSG-BGP, less than 80 nm,  $E = 51 \pm 1.8$  MPa and  $\sigma_{\text{yield}} = 2.8 \pm 0.26$  MPa),<sup>10</sup> indicating a stronger interaction between BPs and gelatin than CSG-BGP with gelatin (Figure 4b). This is not surprising because BPs used in this study were prepared at a much lower temperature and without high temperature processing, therefore they may have less aggregation in gelatin and have more silanol groups on surface, leading to an enhanced interaction between the BPs and gelatin matrix (Figure 3). On the contrary, CSG-BGP were made at a higher temperature and calcinated at 500 °C above to remove toxic nitrate ions, thus is inevitably aggregated and lack of silanol groups. Smaller BPs had larger specific surface area, and thus for a given particle loading, they may provide increasing interaction sites, enhancing the interactions between BPs and gelatin. As a result, both  $E$  and  $\sigma_{\text{yield}}$  of the composite scaffolds were generally found to be greatly improved with decreasing BPs sizes. The  $E$  and  $\sigma_{\text{yield}}$  of BP-14/gel were found to be  $602.3 \pm 73.4$  MPa and  $15.4 \pm 2.5$  MPa, respectively, even higher than those of cancellous bones. It is a bit surprising that the  $E$  of BP-946/gel was higher than BP-580/gel, which might be due to their different porosities.

The mechanical properties of the composite scaffolds were determined not only by the particle size but also by particle loading. The effect of particle loading on the mechanical properties of the scaffolds was also studied. Scaffolds with BP-14 were chosen as a model since they exhibited mechanical properties adjustable to cancellous bones (Figure 5a). It was found that there was a large increase in the  $E$  and  $\sigma_{\text{yield}}$  even at

very low BP-14 content (Table 3). When 2 wt % BP-14 was incorporated, the  $E$  was increased to  $194.2 \pm 45.5$  MPa and  $\sigma_{\text{yield}}$  was increased to  $5.7 \pm 1.2$  MPa, meeting the requirements for the natural cancellous bone. Both  $E$  and  $\sigma_{\text{yield}}$  increased linearly with the BP-14 content (Figure 5b), providing a simple mechanism to adjust the mechanical properties of composite scaffolds.

**3.4. In Vitro Bioactivity.** It is generally accepted that the HA layer formed on the material surface is essential for the bonding between the materials and surrounding bone tissues. These obtained scaffolds were immersed in SBF to investigate the formation of HA. Figure 6 showed the XRD spectra of scaffolds incubated in SBF for 7 (Figure 6a) and 14 days (Figure 6b). It can be seen that all the BP/gel composite scaffolds showed the characteristic peaks of HA after incubating in SBF for 7 or 14 days, whereas the pure gel scaffold did not. For example, the (002) peak at 26°, the (210) peak at 28°, the (211) peak at 32°, the (300) peak at 33°, the (130) peak at 40°, the (222) peak at 47°, and the (213) peak at 49° were all observed from the composite curves,<sup>23</sup> indicating that the BP/gel scaffolds are bioactive. It can also be seen that the intensity of HA became stronger when incubated in SBF for a longer time, suggesting further growth of HA (Figure 6b). It was interesting to find that the bioactivity of the composite scaffolds increased with the decrease in BP size, in agreement with the size effect on bioactivity of BPs.<sup>25</sup> BP-14/gel showed the highest bioactivity among the samples, presumably resulting from the better bioactivity of BP-14 because of its larger specific surface area.

**3.5. Cell Proliferation.** It is important for the artificial bone grafts to have good biocompatibility to stimulate cell adhesion, differentiation, and bone regeneration. The cell compatibility of the BP/gel scaffolds was studied using preosteoblast MC3T3-

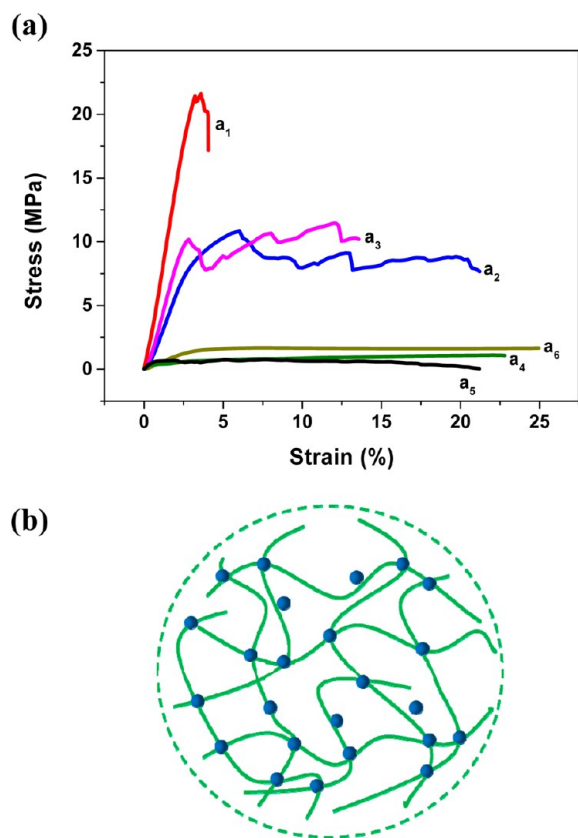


**Figure 4.** (a) Stress–strain curves for BP/gel composite scaffolds under uniaxial compression. (a<sub>1</sub>) BP-14/gel; (a<sub>2</sub>) BP-65/gel; (a<sub>3</sub>) BP-106/gel; (a<sub>4</sub>) BP-580/gel; (a<sub>5</sub>) BP-946/gel; (a<sub>6</sub>) gel. (b) Schematic illustration of interaction between gelatin and BPs in the composite.

E1 cells. BP-14/gel, BP-65/gel, and BP-106/gel composite scaffolds were used as models because they had the similar mechanical properties to the natural cancellous bones. MTT assay was used to investigate the proliferation of MC3T3-E1 cells on BP/gel scaffolds. Gelatin was found to stimulate the growth and proliferation of cells, as shown in Figure 7, where the cell viabilities were larger than 100% compared to the control plate for all culturing intervals examined. Likewise, the proliferation of preosteoblast MC 3T3-E1 cells cultured on BP/gel scaffolds was also significantly higher than that of the control, indicating their good cell compatibility. Additionally, compared to pure gel, BP/gel scaffolds, especially BP-14/gel, even exhibited a better performance on the acceleration of the cell growth within the incubation time, which may be benefited from the bioactivity of the composite. It is not surprising that the cell viability values were partially decreased for BP-14/gel and BP-106/gel at the seventh day, presumably because of the decrease in the dissolution concentration of bioactive glass with the formation of HA.<sup>24</sup> These MTT results demonstrated that the BP/gel scaffolds could facilitate the cell proliferation, and support the cells better than pure gelatin scaffolds as well as the controls, i.e., they are not cytotoxic.

Figure 8 shows the preosteoblast morphology on different scaffolds. It was found that MC 3T3-E1 cells adhered to the wall of both the gel scaffold and the composite scaffolds after 2 days. The cells presented a round shape initially (Figure 8a–d) and became elongated and spindle-like with increasing culture time. After 7 days, MC 3T3-E1 cells adopted a polygonal morphology and spread well on all the scaffolds (Figure 8e–h),

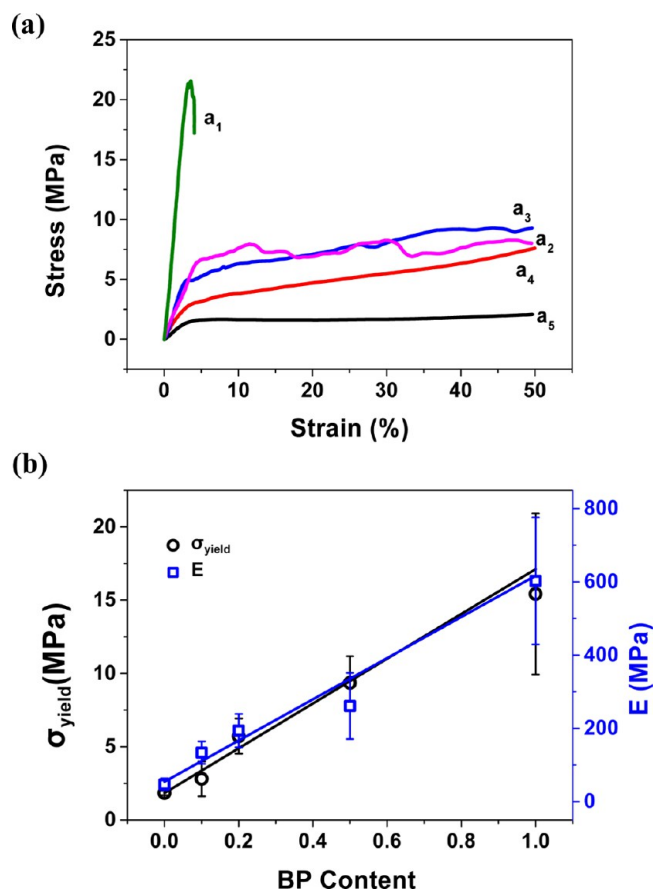


**Figure 5.** (a) Stress–strain curves for BP-14/gel of different content of BP-14 under uniaxial compression. (a<sub>1</sub>) BP-14-1/gel; (a<sub>2</sub>) BP-14-0.5/gel; (a<sub>3</sub>) BP-14-0.2/gel; (a<sub>4</sub>) BP-14-0.1/gel; (a<sub>5</sub>) gel. (b) Effect of BP-14 content on the mechanical properties of the composite scaffolds.

**Table 3. Mechanical Properties of BP-14/Gel Scaffolds at Different Particle Loadings**

| sample          | $E$ (MPa)        | $\sigma_{\text{yield}}$ (MPa) | $\epsilon_{\text{yield}}$ (%) |
|-----------------|------------------|-------------------------------|-------------------------------|
| Cancellous bone | 20–500           | 4–12                          | 5–7                           |
| gel             | $47.2 \pm 16.3$  | $1.8 \pm 0.2$                 | $5.1 \pm 1.2$                 |
| BP-14-0.1/gel   | $133.8 \pm 30.8$ | $2.8 \pm 1.2$                 | $4.2 \pm 1.3$                 |
| BP-14-0.2/gel   | $194.2 \pm 45.5$ | $5.7 \pm 1.2$                 | $3.6 \pm 1.8$                 |
| BP-14-0.5/gel   | $261.0 \pm 90.3$ | $9.4 \pm 1.8$                 | $4.9 \pm 1.2$                 |
| BP-14-1/gel     | $602.3 \pm 73.4$ | $15.4 \pm 2.5$                | $4.0 \pm 0.5$                 |

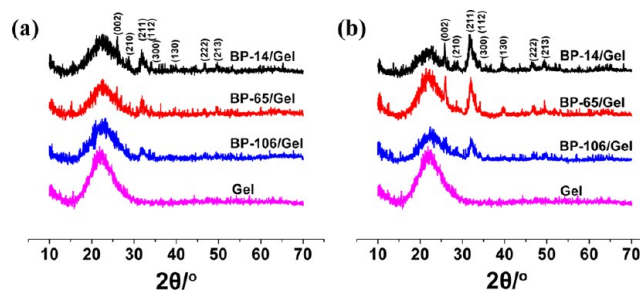


**Figure 6.** XRD spectra of gel and BP/gel scaffolds incubated in SBF for 7 (a) and 14 days (b).

suggesting that MC3T3-E1 cells were able to grow and proliferate well on both gel and BP/gel scaffolds. It is interesting to find that the cells had a better growth on BP/

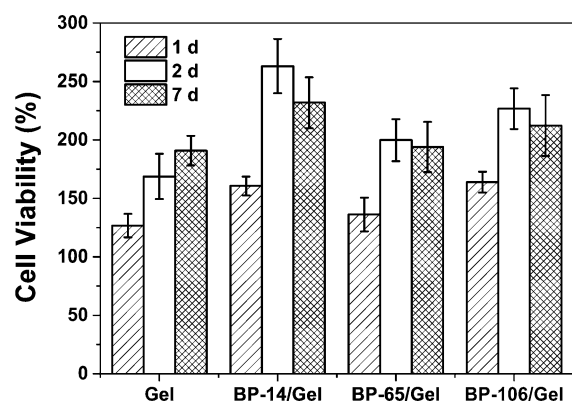


**Figure 7.** MTT assay for preosteoblast MC 3T3-E1 cells proliferation after culturing for different intervals.

gel scaffolds, especially for BP-14/gel, probably because of the increased bioactivity through the incorporation of BPs.

#### 4. CONCLUSION

In summary, we have successfully fabricated macroporous BP/gel nanocomposite scaffolds by using nanosized bioactive silicate glass particles. The bioactive particles (BP) are distributed well in gelatin matrix, thus significantly improved the mechanical properties of composite scaffolds. With the increase in BPs content or decrease in BPs size, both modulus and strength were found to increase, probably resulted from the increasing interfacial area between the nanoparticles and gelatin. The scaffolds with BPs smaller than 100 nm showed similar mechanical properties and porous structure with cancellous bones. The bioactivity was also found to increase with decreasing BPs sizes, evaluated by the formation of HA in SBF, thus the optimized BP/gel composite scaffolds could have both good mechanical properties and cell responses. Prelimi-

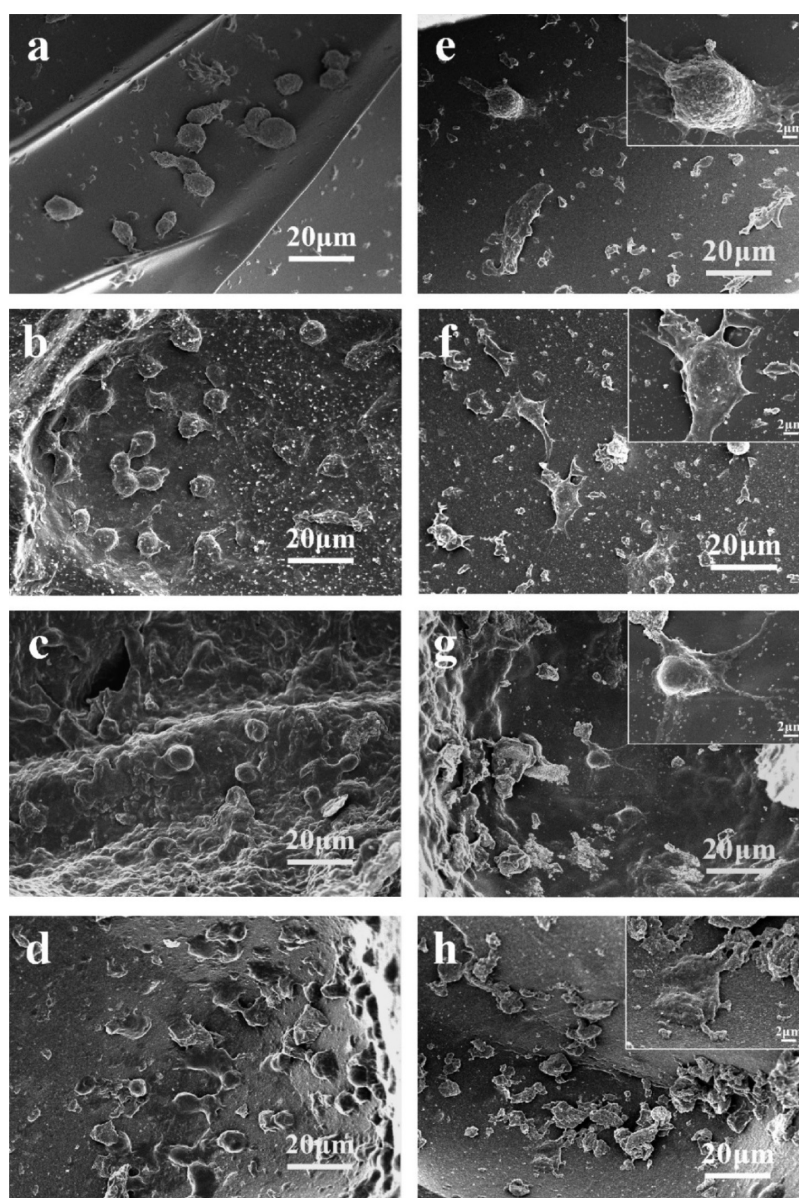


**Figure 8.** SEM images of preosteoblast MC 3T3-E1 cells cultured on gel and BP/gel scaffolds for 2 days: (a) gel; (b) BP-14/gel; (c) BP-65/gel; (d) BP-106/gel; and for 7 days: (e) gel; (f) BP-14/gel; (g) BP-65/gel; (h) BP-106/gel.

nary results on preosteoblasts suggested that cells could adhere, spread, and proliferate very well in the composite scaffolds, making them promising artificial bone grafts.

## AUTHOR INFORMATION

### Corresponding Authors

\*E-mail: liailing@iccas.ac.cn.

\*E-mail: dqiu@iccas.ac.cn.

### Notes

The authors declare no competing financial interest.

## ACKNOWLEDGMENTS

This work was supported by MOST (Project 2012CB933200, 2013DFG52300) and NSFC (Project 51173193, 81202931).

## REFERENCES

- (1) Tavakol, S.; Azami, M.; Khoshzaban, A.; Ragerdi Kashani, I.; Tavakol, B.; Hoveizi, E.; Rezayat Sorkhabadi, S. M. Effect of Laminated Hydroxyapatite/gelatin Nanocomposite Scaffold Structure on Osteogenesis Using Unrestricted Somatic Stem Cells in Rat. *Cell Biol. Int.* **2013**, *27*, 1181–1189.
- (2) Valliant, E. M.; Jones, J. R. Softening Bioactive Glass for Bone Regeneration: Sol–Gel Hybrid Materials. *Soft Matter* **2011**, *7*, 5083–5095.
- (3) Smith, L. A.; Liu, X.; Ma, P. X. Tissue Engineering with Nano-Fibrous Scaffolds. *Soft Matter* **2008**, *4*, 2144–2149.
- (4) Zhang, Q.; Tan, K.; Zhang, Y.; Ye, Z.; Tan, W. S.; Lang, M. In Situ Controlled Release of rhBMP-2 in Gelatin-Coated 3D Porous Poly( $\epsilon$ -caprolactone) Scaffolds for Homogeneous Bone Tissue Formation. *Biomacromolecules* **2014**, *15*, 84–94.
- (5) Azami, M.; Moztarzadeh, F.; Tahriri, M. Preparation, Characterization and Mechanical Properties of Controlled Porous Gelatin/Hydroxyapatite Nanocomposite through Layer Solvent Casting Combined with Freeze-Drying and Lamination Techniques. *J. Porous Mater.* **2010**, *17*, 313–320.
- (6) Kim, H. W.; Kim, H. E.; Salih, V. Stimulation of Osteoblast Responses to Biomimetic Nanocomposites of Gelatin-Hydroxyapatite for Tissue Engineering Scaffolds. *Biomaterials* **2005**, *26*, 5221–5230.
- (7) Mahony, O.; Tsigkou, O.; Ionescu, C.; Minelli, C.; Ling, L.; Hanly, R.; Smith, M. E.; Stevens, M. M.; Jones, J. R. Silica-Gelatin Hybrids with Tailorable Degradation and Mechanical Properties for Tissue Regeneration. *Adv. Funct. Mater.* **2010**, *20*, 3835–3845.
- (8) Zhou, Z. H.; Cao, D. F.; Huang, T. L.; Liu, L. L.; Liu, Q. Q.; Zhao, Y. M.; Ou, B. L.; Zeng, W. N.; Xu, G. R.; Tang, A. P.; Yang, Z. M. Fabrication and Characterization of Gelatin Hyaluronic Acid/Nanobioactive Glass Hybrid Scaffolds for Tissue Engineering. *Mater. Res. Innovations* **2013**, *17*, 532–536.
- (9) Janicki, P.; Schmidmaier, G. What Should be the Characteristics of the Ideal Bone Graft Substitute? Combining Scaffolds with Growth Factors and/or Stem Cells. *Injury* **2011**, *42*, 77–81.
- (10) Mozafari, M.; Rabiee, M.; Azami, M.; Maleknia, S. Biomimetic Formation of Apatite on the Surface of Porous Gelatin/Bioactive Glass Nanocomposite Scaffolds. *Appl. Surf. Sci.* **2010**, *257*, 1740–1749.
- (11) Kothapalli, C. R.; Shaw, M. T.; Wei, M. Biodegradable HA-PLA 3-D Porous Scaffolds: Effect of Nano-Sized Filler Content on Scaffold Properties. *Acta Biomater.* **2005**, *1*, 653–662.
- (12) Jiang, L.; Xiong, C.; Chen, D.; Jiang, L.; Pang, X. Effect of n-HA with Different Surface-Modified on the Properties of n-HA/PLGA Composite. *Appl. Surf. Sci.* **2012**, *259*, 72–78.
- (13) Hong, Z.; Zhang, P.; He, C.; Qiu, X.; Liu, A.; Chen, Li.; Chen, X.; Jing, X. Nano-Composite of Poly(L-lactide) and Surface Grafted Hydroxyapatite: Mechanical Properties and Biocompatibility. *Biomaterials* **2005**, *26*, 6296–6304.
- (14) Zhang, C.; Lu, H.; Zhuang, Z.; Wang, X.; Fang, Q. Nano-Hydroxyapatite/Poly(L-lactic acid) Composite Synthesized by A Modified in situ Precipitation: Preparation and Properties. *J. Mater. Sci.: Mater. Med.* **2010**, *21*, 3077–3083.
- (15) Hench, L. L. The Story of Bioglass. *J. Mater. Sci.: Mater. Med.* **2006**, *17*, 967–978.
- (16) Jones, J. R. Review of Bioactive Glass: From Hench to Hybrids. *Acta Biomater.* **2013**, *9*, 4457–4486.
- (17) Rezwani, K.; Chen, Q. Z.; Blaker, J. J.; Boccaccini, A. R. Biodegradable and Bioactive Porous Polymer/Inorganic Composite Scaffolds for Bone Tissue Engineering. *Biomaterials* **2006**, *27*, 3413–3431.
- (18) Chen, Q. Z.; Boccaccini, A. R. Poly(D,L-lactic acid) Coated 45S5 Bioglass-Based Scaffolds: Processing and Characterization. *J. Biomed. Mater. Res., Part A* **2006**, *77*, 445–457.
- (19) Gentile, P.; Mattioli-Belmonte, M.; Chiono, V.; Ferretti, C.; Baines, F.; Tonda-Turo, C.; Vitale-Brovarone, C.; Pashkuleva, I.; Reis, R. L.; Ciardelli, G. Bioactive Glass/Polymer Composite Scaffolds Mimicking Bone Tissue. *J. Biomed. Mater. Res., Part A* **2012**, *100*, 2654–2667.
- (20) Ma, P. X. Biomimetic Materials for Tissue Engineering. *Biomaterials* **2003**, *24*, 4353–4364.
- (21) Roohani-Esfahani, S. I.; Nouri-Khorasani, S.; Lu, Z. F.; Appleyard, R. C.; Zreiqat, H. Effects of Bioactive Glass Nanoparticles on the Mechanical and Biological Behavior of Composite Coated Scaffolds. *Acta Biomater.* **2011**, *7*, 1307–1318.
- (22) Curtis, A. R.; West, N. X.; Su, B. Synthesis of Nanobioglass and Formation of Apatite Rods to Occlude Exposed Dentine Tubules and Eliminate Hypersensitivity. *Acta Biomater.* **2010**, *6*, 3740–3746.
- (23) Lin, S.; Ionescu, C.; Pike, K. J.; Smith, M. E.; Jones, J. R. Nanostructure Evolution and Calcium Distribution in Sol-Gel Derived Bioactive Glass. *J. Mater. Chem.* **2009**, *19*, 1276–1282.
- (24) Hong, Z.; Liu, A.; Chen, L.; Chen, X.; Jing, X. Mono-Dispersed Bioactive Glass Nanospheres: Preparation and Effects on Biomechanics of Mammalian Cells. *J. Non-Cryst. Solids* **2009**, *355*, 368–372.
- (25) Wang, C.; Xie, Y.; Li, A.; Shen, H.; Wu, D.; Qiu, D. Bioactive Nanoparticle through Post-Modification of Colloidal Silica. *ACS Appl. Mater. Interfaces* **2014**, *6*, 4935–4939.
- (26) Lei, B.; Shin, K. H.; Noh, D. Y.; Jo, I. H.; Koh, Y. H.; Choi, W. Y.; Kim, H. E. Nanofibrous Gelatin-Silica Hybrid Scaffolds Mimicking the Native Extracellular Matrix (ECM) Using Thermally Induced Phase Separation. *J. Mater. Chem.* **2012**, *22*, 14133–14140.
- (27) Liu, X.; Smith, L. A.; Hu, J.; Ma, P. X. Biomimetic Nanofibrous Gelatin/Apatite Composite Scaffolds for Bone Tissue Engineering. *Biomaterials* **2009**, *30*, 2252–2258.
- (28) Bakhtiari, L.; Rezaie, H. R.; Hosseinalipour, S. M.; Shokrgozar, M. A. Investigation of Biphasic Calcium Phosphate/gelatin Nanocomposite Scaffolds as A Bone Tissue Engineering. *Ceram. Int.* **2010**, *36*, 2421–2426.
- (29) Kim, H. W.; Song, J. H.; Kim, H. E. Nanofiber Generation of Gelatin-Hydroxyapatite Biomimetics for Guided Tissue Regeneration. *Adv. Funct. Mater.* **2005**, *15*, 1988–1994.
- (30) Ding, S. J.; Wei, C. K.; Lai, M. H. Bio-Inspired Calcium Silicate-Gelatin Bone Grafts for Load-Bearing Applications. *J. Mater. Chem.* **2011**, *21*, 12793–12802.
- (31) Fu, S. Y.; Feng, X. Q.; Lauke, B.; Mai, Y. W. Effects of Particle Size, Particle/Matrix Interface Adhesion and Particle Loading on Mechanical Properties of Particulate-Polymer Composites. *Composites, Part B* **2008**, *39*, 933–961.
- (32) Chen, J.; Wang, G.; Yu, Z.; Huang, Z.; Mai, Y. Critical Particle Size for Interfacial Debonding in Polymer/Nanoparticle Composites. *Compos. Sci. Technol.* **2010**, *70*, 861–872.
- (33) Li, Z.; Su, Y.; Xie, B.; Wang, H.; Wen, T.; He, C.; Shen, H.; Wu, D.; Wang, D. A Tough Hydrogel-Hydroxyapatite Bone-Like Composite Fabricated in situ by the Electrophoresis Approach. *J. Mater. Chem. B* **2013**, *1*, 1755–1764.
- (34) Hu, X.; Shen, H.; Shuai, K.; Zhang, E.; Bai, Y.; Cheng, Y.; Xiong, X.; Wang, S.; Fang, J.; Wei, S. Surface Bioactivity Modification of Titanium by CO<sub>2</sub> Plasma Treatment and Induction of Hydroxyapatite: In Vitro and In Vivo Studies. *Appl. Surf. Sci.* **2011**, *257*, 1813–1823.
- (35) He, C.; Zhang, F.; Cao, L.; Feng, W.; Qiu, K.; Zhang, Y.; Wang, H.; Mo, X.; Wang, J. Rapid Mineralization of Porous Gelatin Scaffolds

by Electrodeposition for Bone Tissue Engineering. *J. Mater. Chem.* **2012**, *22*, 2111–2119.

(36) Shen, H.; Hu, X.; Yang, F.; Bei, J.; Wang, S. An Injectable Scaffold: rhBMP-2-loaded Poly(lactide-co-glycolide)/Hydroxyapatite Composite Microspheres. *Acta Biomater.* **2010**, *6*, 455–465.

(37) Niemelä, T.; Niiranen, H.; Kellomäki, M.; Törmälä, P. Self-Reinforced Composites of Bioabsorbable Polymer and Bioactive Glass with Different Bioactive Glass Contents. Part I: Initial Mechanical Properties and Bioactivity. *Acta Biomater.* **2005**, *1*, 235–242.